Supplement of Nat. Hazards Earth Syst. Sci., 26, 1745–1766, 2026
https://doi.org/10.5194/nhess-26-1745-2026-supplement

Natural Hazards and Earth System Sciences
Open Access
EGU

Supplement of

The damability function: a probabilistic approach to regional landslide dam susceptibility analysis applied to the Oregon Coast Range, USA

Paul M. Morgan et al.

Correspondence to: Paul M. Morgan (pmmorgan@uw.edu)

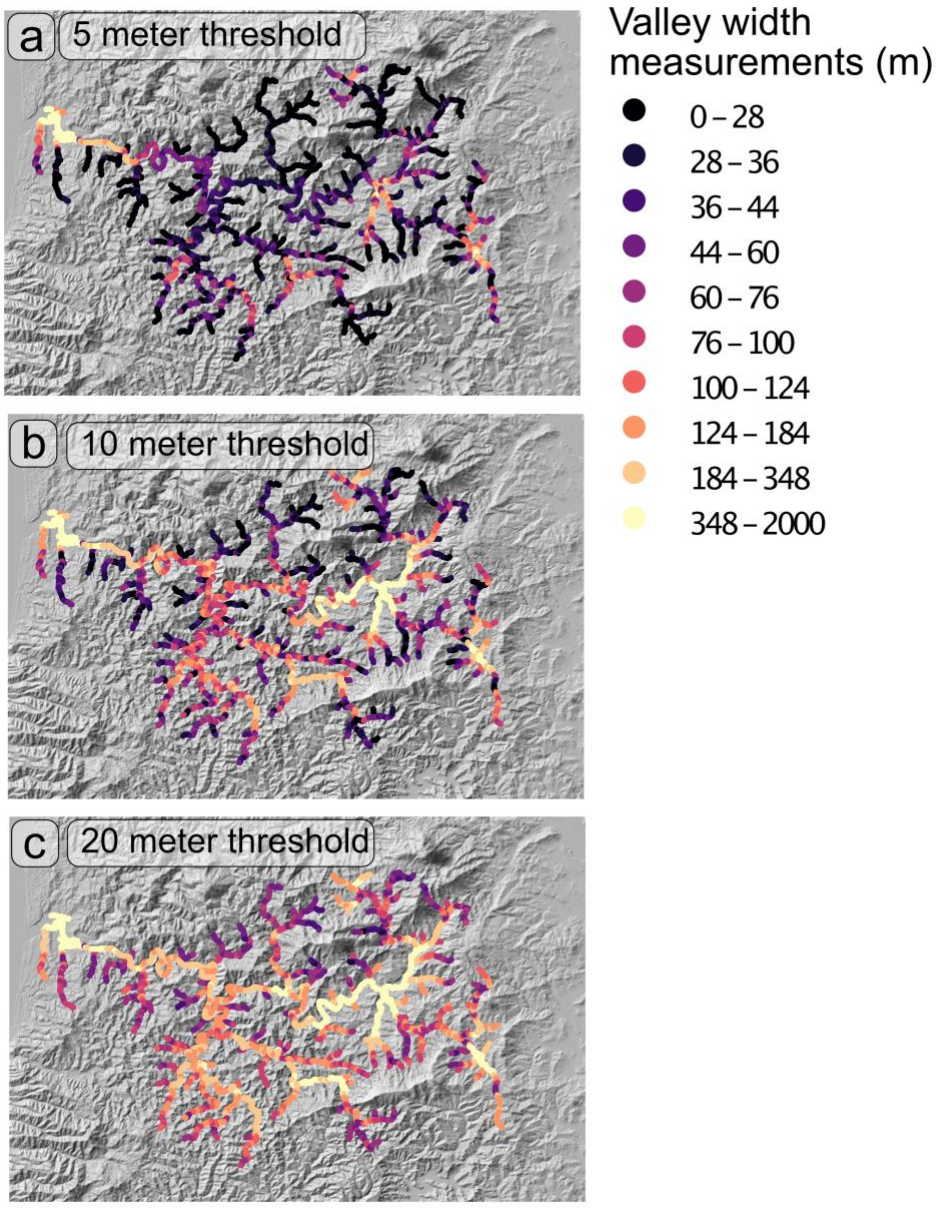

Supplementary Figure S1: Three plots of the Alsea River catchment, depicting valley width measurements with different elevation thresholds to define the valley edges. Note that while the absolute value of the widths does change, increasing width values with increasing threshold value, the spatial distribution does not. Locations with lower or higher width values remain constant. The elevation threshold is set to match the data from May et al. 2013 (Supp. Fig. S2).

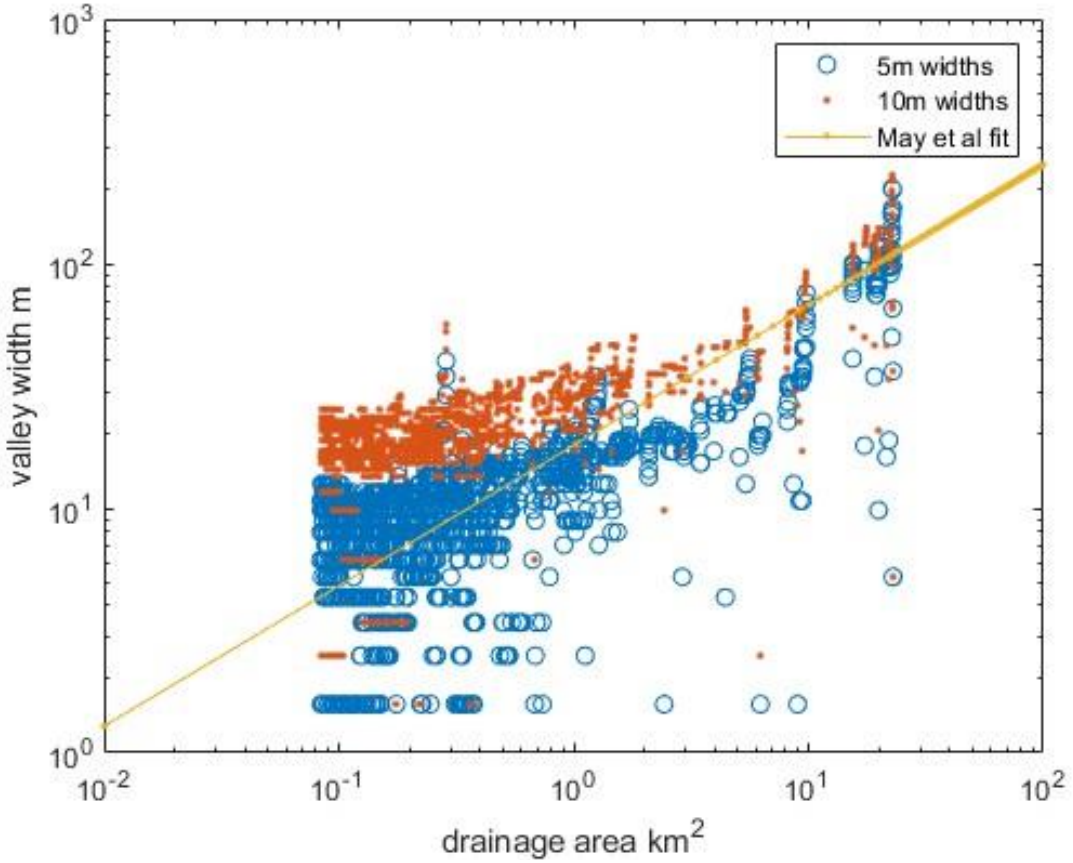

Supplemental Figure S2: Drainage area to valley width relationship plotted for the Harvey Creek drainage. After May et al. (2013). The yellow line is the data fit to the measurements from May et al. 2013 while the red dots and blue circles represent valley widths calculated with two different elevation thresholds. Note that the 10m threshold elevation values match the fit line better for drainage areas down to ~10 square km. McMeckin (2022) compared Topographic position index (TPI) based and threshold (slope and elevation) based methods and found both were acceptable where the methods succeeded. Most landslide dam susceptibility studies factor in some form of the river or valley geometry (Fan et al., 2020). We do not argue that the difference in valley width measurement method is important. Measuring valley width, through elevation thresholds matches intuition of blocking water flow to form lakes, though we have not explored differences between this approach and a river width only, or a morphological classification based approach.

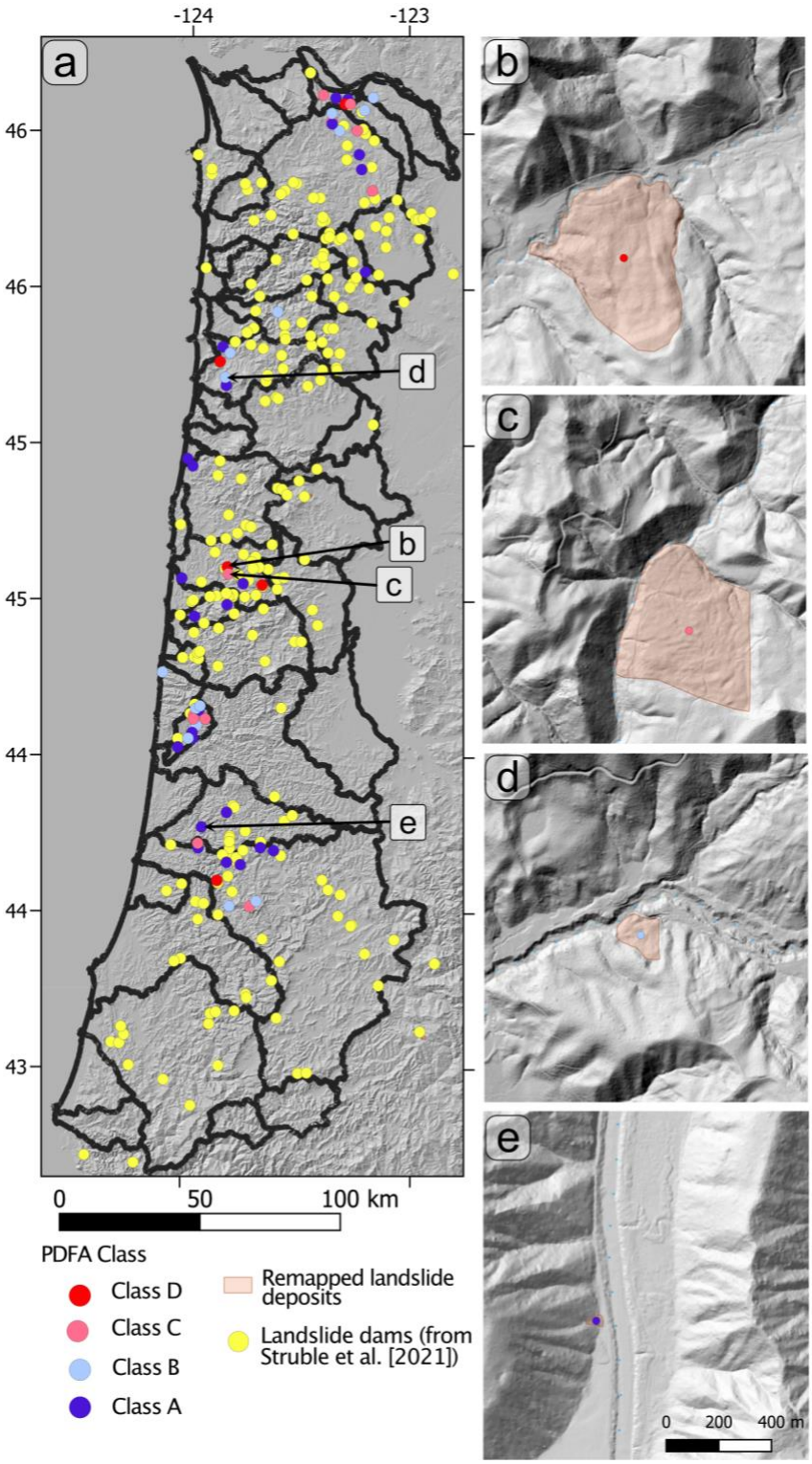

Figure S3: Examples of landslides within the dam/non-dam inventory used to calibrate the OCR DFD function. A) shows locations of landslide dams used for the DFD function regression. b) - e) examples of type 4 -type 1 landslides respectively.

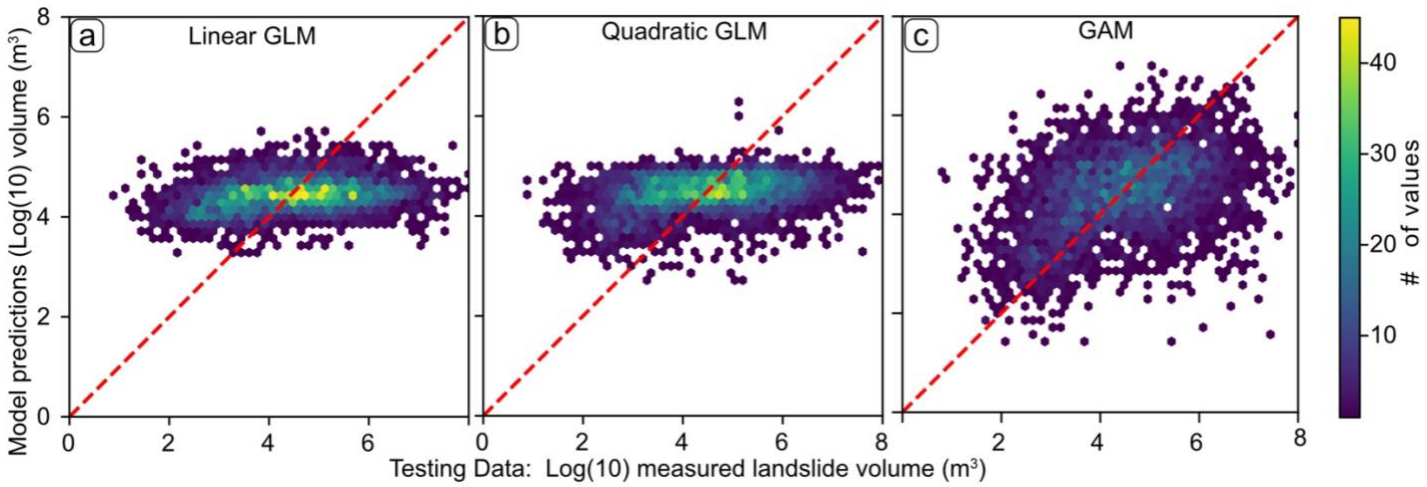

Figure S4: Comparison of measured landslide volumes and model predictions ultimately deemed unsuccessful. These are blind predictions of volume for the 20% of the inventory withheld from model development. a) shows the predictions from a general linear model limited to linear fits, b) shows the predictions from a general linear model predicted with quadratic fits, and c) shows the predictions from a general additive model. All models trained with slope unit extracted local parameters, for radially extracted predictor results see Supp. Fig. S5.

Predictor variable extraction technique	GAM	GLM1	GLM4
Radial mean	1.1237	0.9767	0.9546
Slope unit	0.9615	1.075	1.051

Table S1: Statistical regression model results presented as the IMMSE (improved minimum mean squared error).

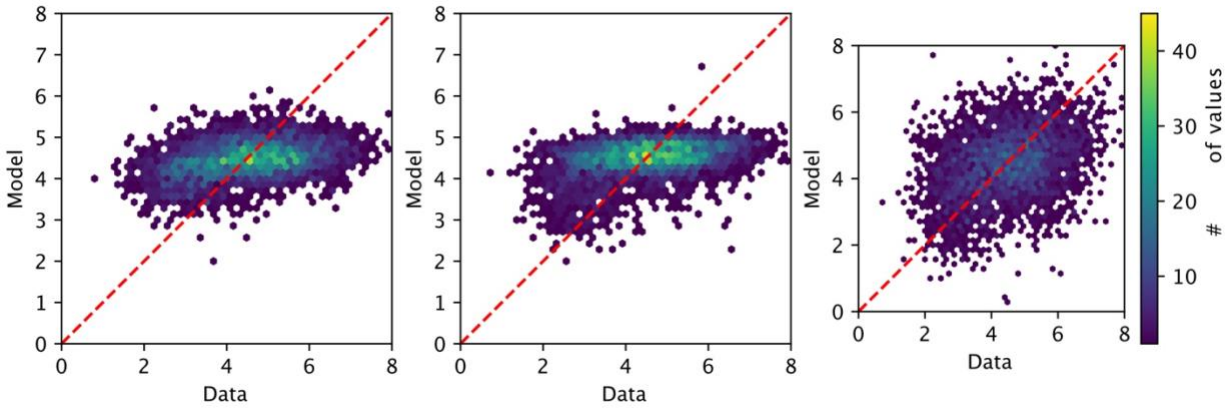

Figure S5: Comparison of measured landslide volumes and regression model predictions. These are blind predictions of volume for the 20% of the inventory withheld from model development. a) shows the predictions from a general linear model limited to linear fits, b) shows the predictions from a general linear model predicted with quadratic fits, and c) shows the predictions from a general additive model. As opposed to Fig. S4 these are results calculated from predictor variables extracted using a moving window with a 500 m radius. More methodological differences between this study and previous studies that may account for the differences include: The target variable in our study is individual landslides whereas Moreno et al. (2022) aggregated all landslides within a slope area, and Lombardo et al. (2021) used the maximum landslide area per slope unit. Additionally, these previous studies were limited to landslide area, whereas we use landslide volumes. The additional complexity stepping from area to volume may make a difference.

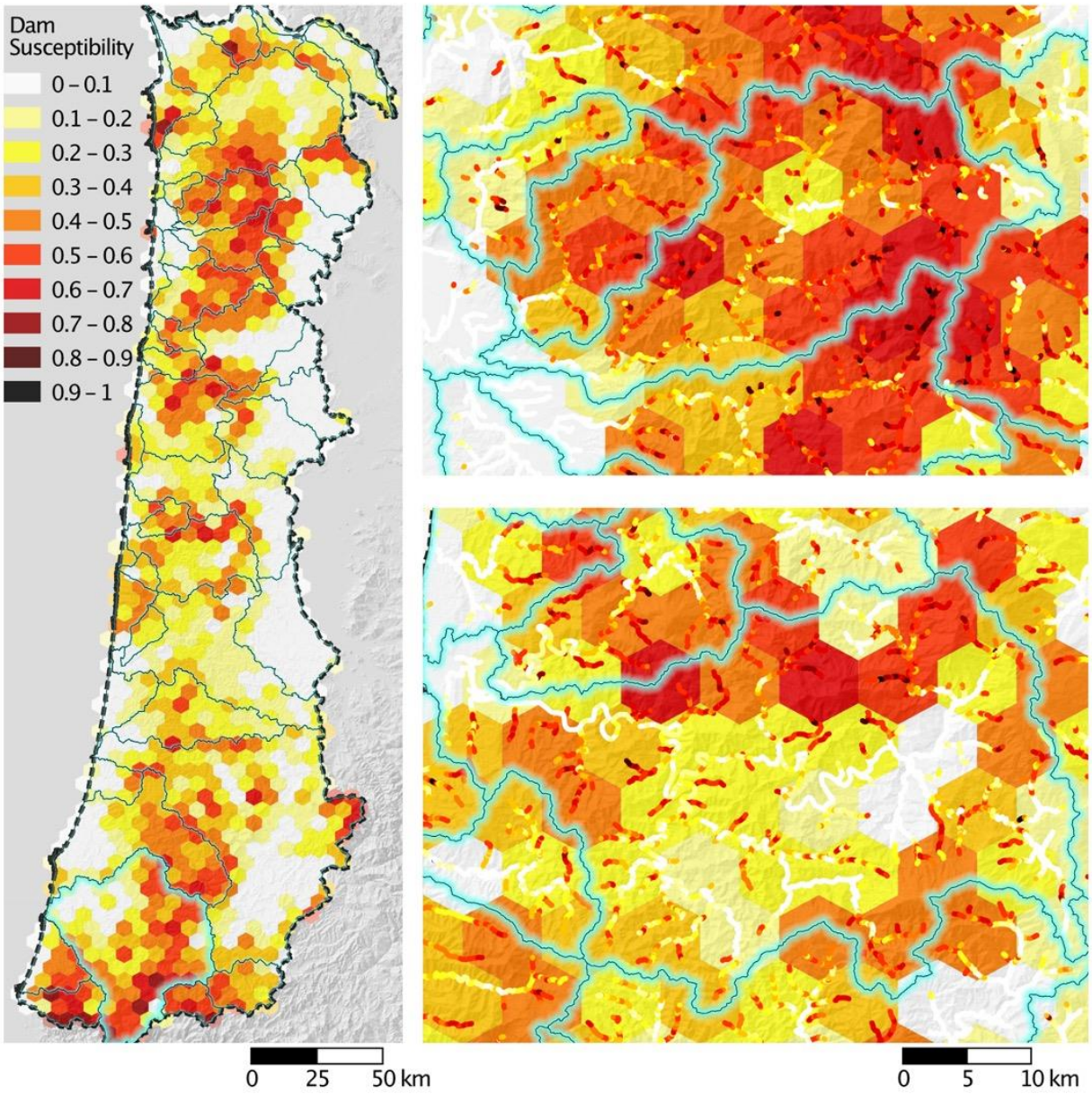

Supplemental Figure S6: a) Damability value estimates for the Oregon Coast Range. a) shown as averages over ~6 km across or ~30 km^2 area hexagons as well as for individual 100 m long river stretches. b) Wilson and c) Alsea catchments. Note that changes in the values is minimal between the 'damability' values plotted here and the dam susceptibility values plotted in Fig. 8

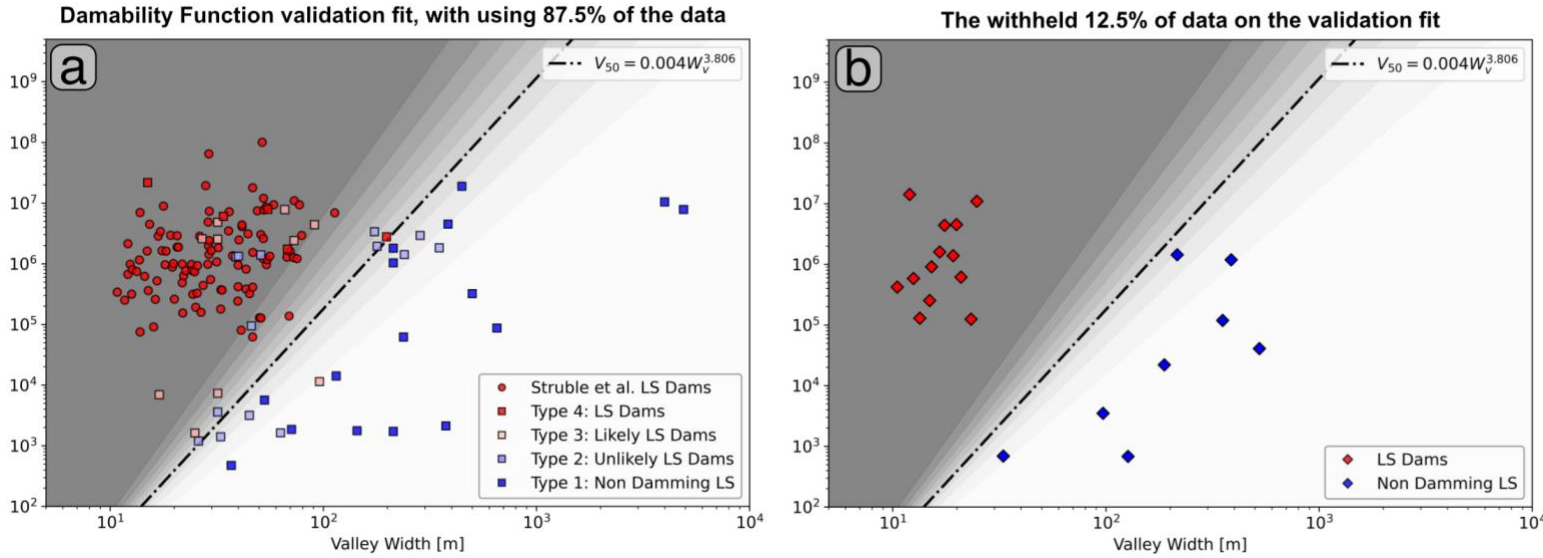

Supplementary Figure S7: Validation of the damability function fits. a) depicts the damability function fit to a training dataset with 12.5% of the dam forming datapoints and the dam non-forming datapoints randomly withheld. Note that the function fit is very similar to the function plotted in Fig. 6. b) depicts the withheld datapoints plotted on the validation fit from a). Note that all points lay on the matching side of the V_{50} line.

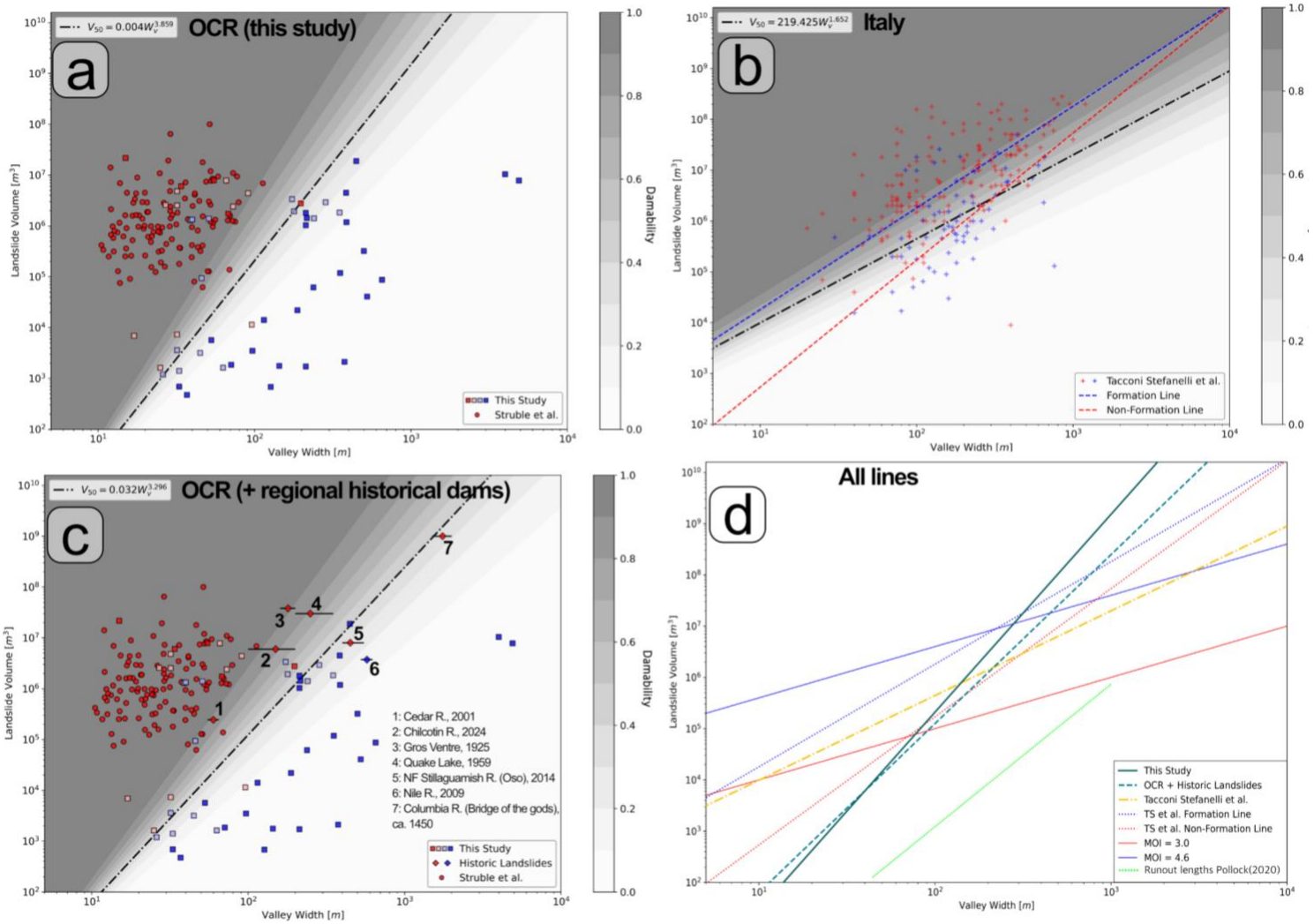

Supplementary Figure S8: Damability function fits for various datasets. a) is a repeat of Fig. 6, b) is the logistic damability function regression results for the landslide dam/non-dam dataset presented in (Tacconi Stefanelli et al., 2015). Also plotted are the V_{50} line of the regression damability function, and the formation and non-formation lines used in Tacconi Stefanelli et al. (2020). c) is the same as a), but with the addition of several notable recent and historic landslide dams within the Northwest US. The damability function is refit to include the notable landslides, this illustrates that the damability logistic regression is flexible to the input of new data, however the new fit is not used in our study, since the notable landslides are from outside the study area. d) has all lines in the volume valley width plot referenced in this study: dark grey is the V_{50} line from plot a) this study, dark grey dashed is the V_{50} line from plot c, note that it has a shallower slope than the line used in this study, Yellow dashed is the V_{50} line from plot b), blue and red dashed are the formation and non-formation lines used as the primary damability functions in Tacconi Stefanelli et al., (2020), solid red and blue lines represent the upper and lower edges of Morphological Obstruction Index (MOI) values claimed to mark the edges of the dam forming and non-forming domains in Tacconi Stefanelli et al., (2016), Light green dashed line represents the global regression to fit landslide volume to runout relationships of Pollock (2020), note that in this line the length scale is slide runout rather than valley width.

The damability functions work better at separating the data into formation and non-formation domains than the Morphological Obstruction Index (MOI) metric numbers itself, which is calculated as the ratio between log width and log volume (Figure S4) (Carlo Tacconi Stefanelli et al., 2016). The slopes of lines defined by constant MOI values are 1 in the log-log space, which is too shallow to accurately capture the domains represented by the data. We suggest that the MOI values be rethought with an exponent added, or that only the dam formation domain functions be considered going forward.

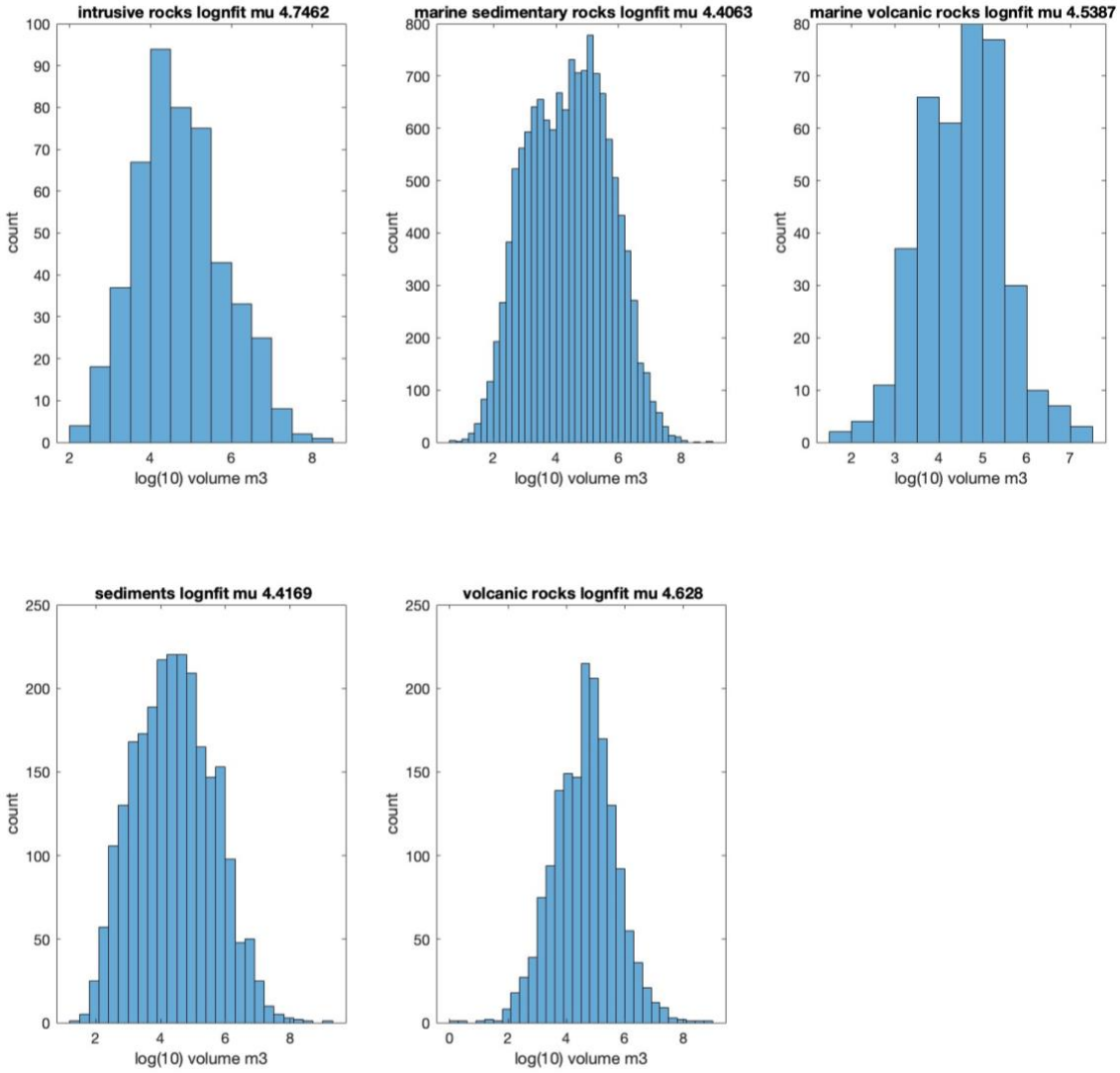

Supplementary Figure S9: Histograms of the SLIDO landslide log volumes (Franczyk et al. 2020) with respect to rock type. Note that the lognormal mean of the distributions is similar for all rock types. Minimum number of landslides of 200 required to be listed in this plot.